

RESEARCH ARTICLE

Design of a multi-story steel building according to the Turkish Building Earthquake Codes: TBEC-2007 vs. TBEC-2018

İbrahim Emrah Katmer¹, Tuğçe Sevil Yaman^{2*}

- ¹ Directorate of Development and Urbanization, Kilis Municipality, Kilis, Türkiye
- ² Mersin University, Department of Civil Engineering, Mersin, Türkiye

Article History

Received 5 May 2023 Accepted 8 July 2023

Keywords

Multi-story steel building Concentrically braced steel frames

Turkish Building Earthquake Code 2007

Turkish Building Earthquake Code 2018

Abstract

People have built structures to survive and to meet their shelter needs. While buildings had progressed horizontally at first, the increase in population and shrinkage of spaces over time led the construction industry to build multi-story buildings. In the research, the Turkish Building Earthquake Code 2007 (TBEC-2007) and the Turkish Building Earthquake Code 2018 (TBEC-2018) were extensively examined and an 8-story steel business center building having high ductility levels in both directions and consisting of concentrically braced steel frames was designed according to the two earthquake codes. The Equivalent Static Method was utilized while designing according to the codes. For structural elements' dimensioning, the Regulation on Design, Calculation, and Construction Principles of Steel Structures principles were followed and the Load and Resistance Factor Design Method was utilized. After performing the analyses of the building according to both earthquake codes, the effects of the code differences on the system periods, earthquake loads, lateral displacements, the story drifts, second-order effects, A1 type torsional irregularities, B2 type stiffness irregularities, and dimensioning of the elements were evaluated in detail. It was observed that in TBEC-2018 compared to TBEC-2007, the structure's coordinates are determined more specifically while identifying the earthquake load, more sensitive soil options are presented, separate calculations according to building height are performed, and base shear forces are smaller. Moreover, it was deduced that there was no significant variance between the codes in terms of calculations of building importance coefficient, natural vibration period, story drifts, and irregularities.

1. Introduction

One of the most important variables in the design of tall buildings is safety. The behavior of the building under horizontal and vertical loads is extremely important for safety. Approximately 90% of Türkiye's land is in the earthquake zone. After the 1999 Kocaeli earthquake in Türkiye, the issue of security, especially in multi-story buildings, has been discussed and the use of steel structures as an alternative to reinforced concrete structures has been considered.

^{*} Corresponding author (<u>tsevilyaman@mersin.edu.tr</u>)

When the whole building is thought, the load transferred to the foundation is also reduced due to the low ratio of the self-weight of steel to the total load. The most important effect of this situation on the building is that it provides an advantage against earthquakes. The high strength, easy repair, and high ductility of steel compared to reinforced concrete are some of the other reasons for preferring steel, especially in earthquake zones. Besides, being fabricated and being completely recyclable are some prominent features that make steel stand out [1]. In addition, steel's tensile strength is equal to its compressive strength and it has a high modulus of elasticity.

Some prominent studies demonstrating the state of the field on the research topic are summarized below: The seismic performance of concentrically braced steel frames in multi-story buildings with mass irregularity was studied by Tremblay and Poncet [2]. The equivalent static method and the response spectrum analysis method were utilized to design the systems according to the 2005 NBCC bases. The mass irregularity conditions were observed to have a little negative effect on the performance of systems designed with the static method. Uriz and Mahin [3] performed research on the seismic behavior of concentric braced frames and buckling restrained braced frames. A reliability framework was employed and an experimental program was conducted to help improve the modeling of the systems.

Multi-story steel frames with self-centering braces were investigated by Qiu and Zhu [4] by pushover and incremental dynamic analyses. They found out that the self-centering capability of the frames was the main advantage over buckling restrained and conventional steel-braced frames. The seismic behavior of steel buildings with hybrid braced frames containing buckling restrained braces and conventional braces was examined by Chao et al. [5]. Nonlinear time-history analyses were realized. It was seen that the usage of buckling restrained braces at only lower levels of the hybrid system gave similar results as buckling restrained brace frames.

Shen et al. [6] realized analytical research to examine the seismic performance of concentrically braced frames with and without brace buckling. It was concluded that the buckling-controlled braces may reduce story drift response, prevent weak beam yielding, and avoid fracturing in braces. The shaking table test and numerical modeling of a steel frame system were realized by Avcı and Alemdar [7]. It was observed that the effect of semi-rigid connections on the system was significant. The analytical and test results matched well.

Annan et al. [8] tested a modular steel-braced frame and a regular concentrically-braced frame under reversed cyclic loading and compared the frames' behaviors. An analytical model was verified using the test results. Kirruti and Pekrioglu Balkis [9] studied the seismic performance of concentric steel bracings in high-rise reinforced concrete frames. A moment-resisting frame, three uniformly braced frames, and a combined brace frame were analyzed. The X-braced system was found to be the best concentric system having the best overall performance.

A 35-story steel building of normal ductility level was designed by Serttaş [10] according to the Specification for Structural Steel Buildings (ANSI/AISC 360-10) based on İstanbul Tall Buildings Earthquake Code (ITBEC) and İstanbul Tall Buildings Wind Code (ITBWC). It was seen that the element load values were higher in the earthquake effect-included combinations. A study to design four ductile steel moment-resisting frame buildings having 5, 10, 15, and 20 stories according to the National Building Code of Canada (NBC) was performed by Yousuf ve Bagchi [11]. Real ground motion records were utilized to investigate the nonlinear dynamic response of the buildings. It was deduced that the presence of infill walls, the nature of ground motion records, and the methods for scaling them affected the performance.

Yousuf ve Bagchi [12] researched to perform a non-linear static pushover analysis of a 20-story moment-resisting steel frame building using simulated and real ground motion records. The direct displacement-based design method was found to be more proper to achieve the performance-based design of a building. Seismic design procedures of high-rise buildings were described by Nakai et al. [13] Designs of a 100 m high reinforced concrete building and a 300 m high steel building were compared by realizing nonlinear analyzes

using. Nateghi and Tabrizi [14] observed that the interaction between adjacent buildings caused changes in the nonlinear response, damage, and performance level depending on the dynamic properties of such structures and the input motion's frequency.

A 9-story steel building with a high ductility level was designed by Dağdeviren [15] according to TBEC-2007. It was found that the study realized according to the TBEC-2007 was compatible with the FEMA-356 and the ATC-40 approaches. The Nonlinear Push-Over Analysis Method was utilized by Atalay [16] for the analyses of two models of a steel building having different bracings. Performance analysis was done according to the TBEC-2018. It was concluded that the eccentrically braced system was preferable.

Kor and Ozcelik [17] designed a set of concentric X-braced steel frames of six different story heights according to the TBEC-2018 and formed a nonlinear numerical model. Afterward, nonlinear static and dynamic analyses were performed. Finally, the systems' behaviors were interpreted and the fragility curves were drawn. Yıldızhan Sağer and Temel [18] designed concentrically braced two 5-story and two 10-story steel buildings according to the TBEC-2018. The Equivalent Static Method was utilized for the 5-story buildings, and the Mode Combination Method was used for the 10-story structures. Resultingly, it was observed that the TBEC-2018 boundary condition values were easily achieved in the concentrically braced systems.

In this research, initially, a comprehensive investigation of the TBEC-2007 [19] and the TBEC-2018 [20] was performed and the differences between the two earthquake codes and the novelties brought by TBEC-2018 [20] were examined.

In Türkiye, there are mostly reinforced concrete structures as multi-story buildings. In this study, steel structures, which have many advantages against earthquakes, were examined. The studies carried out so far are mainly on reinforced concrete structures, at the time of the research, there were only a few studies on the design of multi-story steel structures according to the TBEC-2007 [19]. There was no study on the design of multi-story steel structures based on comparison and sizing according to the TBEC-2007 [19] and the TBEC-2018 [20] earthquake codes. For this reason, the study is of high original value.

In the study, an 8-story steel building having high ductility in both directions, comprising concentrically braced steel frames was designed with respect to the considered earthquake codes. The building's behavior under seismic loads was evaluated and the results were compared. The effects of the code differences were studied in terms of the structural system periods, seismic loads, lateral displacements, story drifts, irregularities, and dimensioning of all the structure's elements.

Design of the multi-story steel building according to the TBEC-2007 and the TBEC-2018

2.1. Structural system and design method

A steel business center building with 8 stories having high ductility in both directions and comprising concentrically braced steel frames were designed with respect to the TBEC-2007 [19] and TBEC-2018 [20] earthquake codes. To observe the impact of the code variance, the system periods, earthquake loads, lateral displacements, story drifts, irregularities, and elements' dimensioning were evaluated. The 8-story steel building was modeled and analyzed with the SAP2000 [21] structural analysis program.

The floor plan of the 8-story steel building designed in the research is presented in Fig. 1. Views of the building model from different aspects are shown in Figs. 2-4. While designing the building according to TBEC-2007 [19], typical elements were dimensioned according to the Regulation on Design, Calculation, and Construction Principles of Steel Structures (RDCCPSS-2018) [22] and the TBEC-2007 [19] principles. Likewise, while designing according to TBEC-2018 [20], typical elements were dimensioned based on the RDCCPSS-2018 [22] and the TBEC-2018 [20] rules. The Load and Resistance Factor Design (LRFD)

Method specified in the RDCCPSS-2018 [22] was used in the design of the building for both earthquake codes. Design with the LRFD Method is based on the principle that for all structural elements the design strength, ϕR_n , is equal or greater than the required strength, R_u , calculated under the load combinations envisaged for this design method.

The lateral load-bearing system of the building examined in the study in both earthquake directions consisted of concentrically braced steel frames with high ductility levels given in TBEC-2007 [19] and TBEC-2018 [20]. The building, designed as a business center, had dimensions of 35×24 m and a living area of 840 m^2 . The story height was 3 m for all stories. The building had five bays in the x direction and all bays' spacings were 7 m. Likewise, the building consisted of 4 bays in the y direction and the spacings of all bays were 6 m. The columns' supports to the foundation were considered fixed support. The slabs, on the other hand, consisted of cast-in-situ reinforced concrete composite slab systems connected to the steel beams. The secondary intermediate beams connected to the main beams were placed at 2 m spacings.

The structural members were dimensioned using European norm profiles by selecting IPE profiles for secondary beams, HEA profiles for columns and frame beams, and box profiles for bracings). In the design of the system, S275 structural steel was utilized. According to the RDCCPSS-2018 [22], the characteristic yield stress of S275 structural steel is $F_y = 275 \text{ N/mm}^2$, the characteristic tensile strength is $F_u = 430 \text{ N/mm}^2$, and the modulus of elasticity is $E = 200000 \text{ N/mm}^2$.

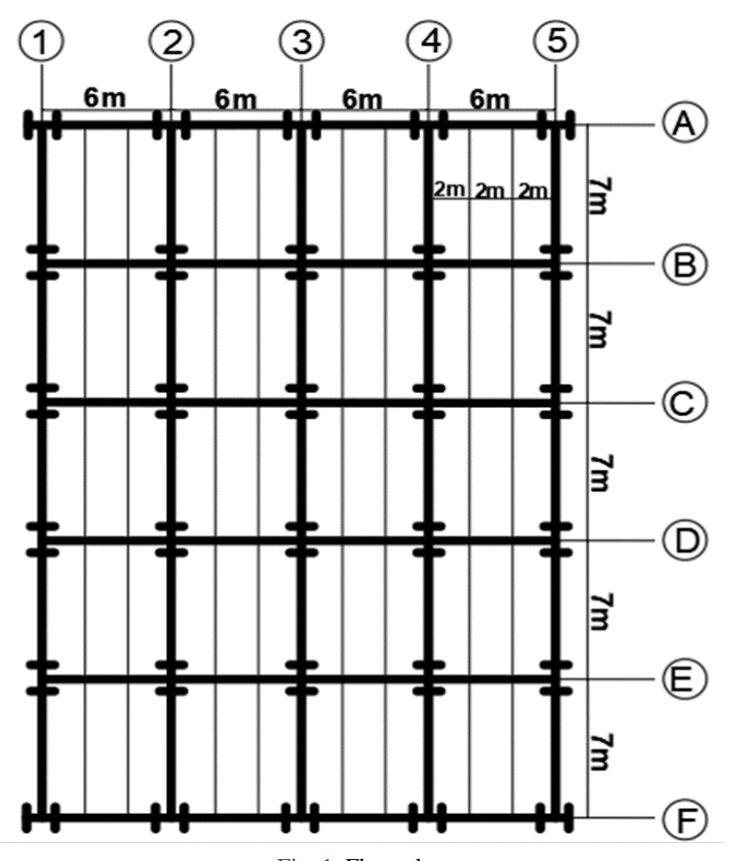


Fig. 1. Floor plan

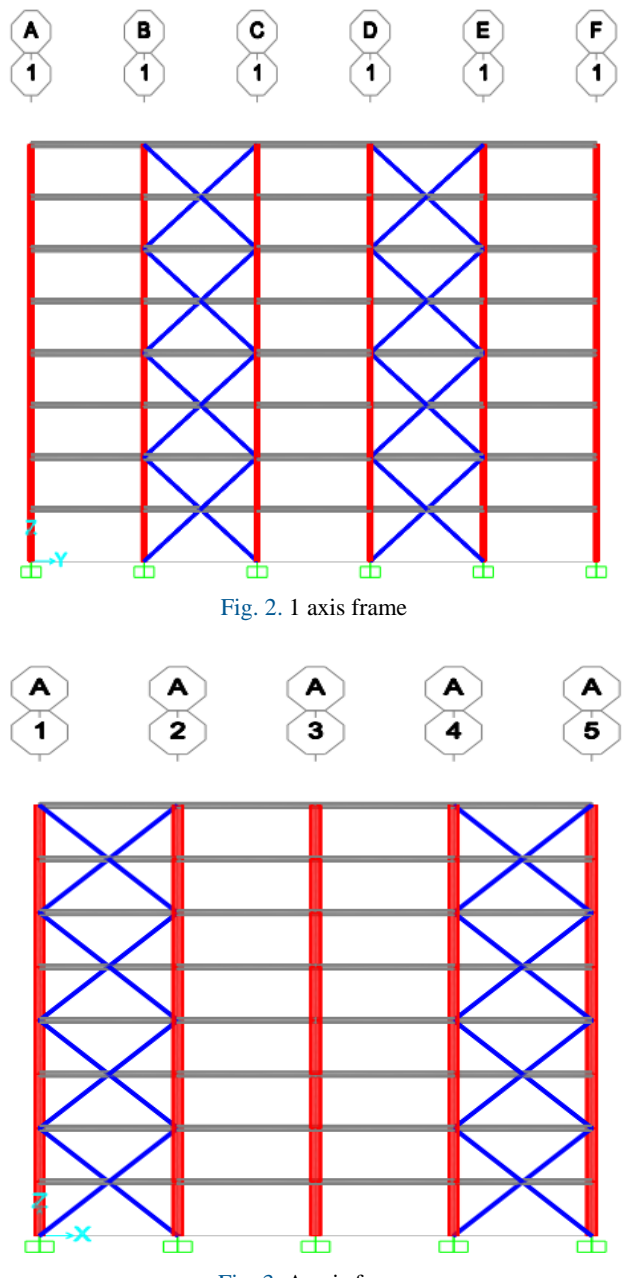


Fig. 3. A axis frame

In the research, the Equivalent Static Method was used while designing according to both earthquake codes. In the Equivalent Static Method, the load that will affect the building is determined according to properties such as local soil class, earthquake zone, building usage type, structural system type, natural dominant period of building, and building weight. There are various limits in the usage of the Equivalent Static Method in the TBEC-2007 [19] and TBEC-2018 [20] earthquake codes, such as the total height of the building, earthquake zone, and irregularities of the building in plan and in vertical. In the study, modeling was performed by using the SAP2000 [21] structural analysis program. The building model was formed in

the SAP2000 [21] program and the diaphragm was assigned for all stories. The loads acting on the building were determined and loads for all stories, i.e. dead load, live load, snow load, and wind load, were defined.

In the earthquake loading, first fictitious load was determined and then the loading was applied to all stories according to story weights and story heights. The natural vibration periods were calculated according to the story displacement values under the loading. Then, by finding the base shear forces, equivalent earthquake loads were calculated and earthquake loads were applied to all stories. After the application of all the loads to the building, the story drifts, second-order effects, A1 type torsion, and B2 stiffness irregularities were checked using the displacement values resulting from the earthquake loads applied to all stories. Afterward, load combinations were defined according to the TBEC-2007 [19] and TBEC-2018 [20] earthquake codes' principles, and these load combinations were applied to the building. Eventually, the shear force, moment, and axial force values for the most critical elements were obtained. In addition, the dimensioning was carried out in a way that complies with the bases of the RDCCPSS-2018 [22].

2.2. Structural system and design method

The design steps of the 8-story steel building composed of concentrically braced steel frames by the Equivalent Static Method according to the TBEC-2007 [19] earthquake code are described in this section. The system periods, earthquake loads, lateral displacements, story drifts, irregularities, and dimensioning of the system elements were examined.

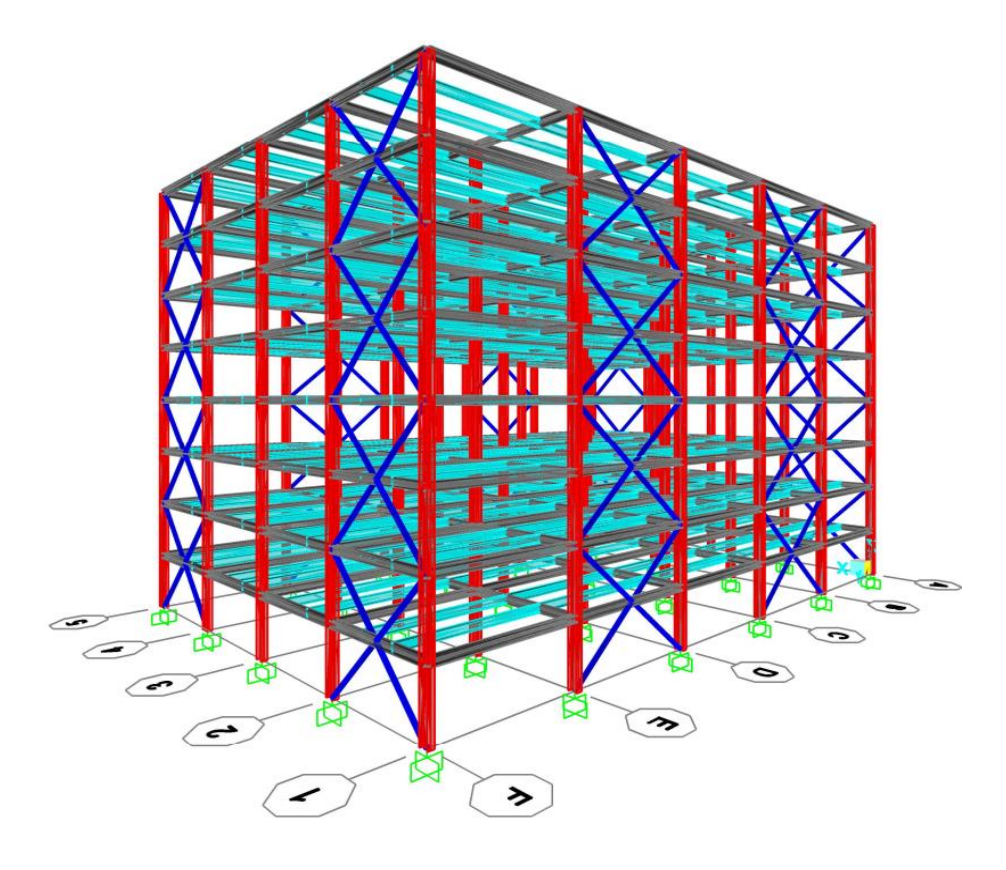


Fig. 4. 3D general view

2.2.1. Vertical loads

Roofing and story slab loads are calculated as follows:

Roofing loads:

Covering: 0.5 kN/m^2 Trapezoidal Sheet + RC Flooring: 2.1 kN/m^2 Isolation: 0.2 kN/m^2 Plaster + Installation: 0.4 kN/m^2 Steel Construction: 0.9 kN/m^2 Total Dead Load: $G = 4.1 \text{ kN/m}^2$

Live Load: $G = 4.1 \text{ kN/m}^2$ $Q = 2.0 \text{ kN/m}^2$ Parapet Load: $G_d = 2.0 \text{ kN/m}^2$

Story slab loads:

Covering: 0.5 kN/m^2 Trapezoidal Sheet + RC Flooring: 2.1 kN/m^2 Interior Walls: 0.9 kN/m^2 Plaster + Installation: 0.4 kN/m^2 Steel Construction: 1.1 kN/m^2

Total Dead Load: $G = 5.0 \text{ kN/m}^2$ Live Load: $Q = 2.0 \text{ kN/m}^2$ Parapet Load: $G_d = 3.0 \text{ kN/m}^2$

Spectrum Characteristic Periods:

Dead and live loads in stairs and elevator areas were assumed to be equal to dead and live loads in other parts of the slab.

2.2.2. Earthquake characteristics

For a system consisting of concentrically braced steel frames with high ductility levels in both directions:

 $T_{\rm A} = 0.1 \, {\rm s}$, $T_{\rm B} = 0.3 \, {\rm s}$

•	Building Usage Purpose:	Business Center
•	Local Soil Class:	ZB
•	Earthquake Zone:	Zone 2
•	Effective Ground Acceleration Coefficient (A_0):	0.3
•	Building Importance Factor (<i>I</i>):	1
•	Soil Group:	A
•	Local Soil Class:	Z1

• Structural System Behavior Coefficient (*R*): 5

2.2.3. Determination of the first natural vibration period of the building

According to the Equivalent Static Method in the TBEC-2007 [19] earthquake code Part 2.7.4.1, the first natural vibration periods of the building in both earthquake directions are calculated by

$$T_1 = 2\pi \left(\frac{\sum_{i=1}^{N} m_i \cdot d_{fi}^2}{\sum_{i=1}^{N} F_{fi} d_{fi}} \right)^{1/2}$$
 (1)

The value of the story mass, m_i , is determined by

$$m_i = \frac{w_i}{g} = \frac{1}{g} \left[G_i + nQ_i \right] \tag{2}$$

The story weight and story mass of the first story are calculated by Eq. (3), where n is taken as 30 for the first story according to Table 2.7 of the TBEC-2007 [19].

$$w_i = \text{Area}(G_n + nQ_n) + \text{Perimeter}(G_d)$$
(3)

By performing the calculations in the same way for other stories, story weights, and story masses of all stories were found. Fictive forces, F_{fi} , proportional to the story weights, and the story heights were calculated by Eq. (4) for all stories.

$$F_{fi} = F_0 \left(\frac{m_i H_i}{\sum_{j=1}^N m_j H_j} \right) \tag{4}$$

In this equation, F_0 represents any chosen load and it was taken as 1000 kN. The F_{fi} forces in Table 1 were applied to story mass centers in the X and Y directions and story displacements were obtained.

Natural vibration periods $T_p^{(x)}$ and $T_p^{(y)}$ were calculated by Eq. (5).

$$T_p = 2\pi \left(\frac{\sum_{i=1}^{N} m_i \cdot d_{fi}^2}{\sum_{i=1}^{N} F_{fi} \cdot d_{fi}} \right)^{1/2}$$
 (5)

2.2.4. Total equivalent static lateral force calculation

The building designed according to Table 2.6 of the TBEC-2007 [19] was in the earthquake zone 2 and there were no torsion and B2 (soft story) irregularities in the structural system. For that reason, the Equivalent Static Method was applied. The total equivalent static lateral force was calculated using Eq. (6).

$$V_t = \frac{WA(T_1)}{R_a(T_1)} \ge 0.10A_0 IW \tag{6}$$

Base shear force was calculated as below for the X earthquake direction: Since $T_{1,x} = 0.899 > T_B = 0.30$, the spectrum coefficient S(T) was determined by Eq. (7) according to the TBEC-2007 [19] Part 2.4.3.

$$S(T) = 2.5(\frac{T_B}{T})^{0.8} \quad S(T_{1,x}) = 2.5(\frac{0.3}{0.899})^{0.8} = 1.039$$
 (7)

The spectral acceleration coefficient A(T), to be taken as a basis in the earthquake load calculation, was obtained by Eq. (8) given in the TBEC-2007 [19] Part 2.4.

$$A(T) = A_0 I S(T) \tag{8}$$

Since $T_{1,x} = 0.899 > T_A = 0.10$, the earthquake load reduction coefficient $R_a(T)$ was calculated by Eq. (9) in the TBEC-2007 [19] Part 2.5.

$$R_{a}(T) = R \tag{9}$$

203	Katmer and Yaman
ZU.)	Natifici alia falliali

Story	F_{fi} (kN)	$m_i(kNs^2/m)$	$d_{fi(x)}(\mathbf{m})$	$m_i d_{fi(x)^2}$ (kNms ²)	$F_{fi}\times d_{fi(x)}\ (kNm)$
Roof	179.8018	395.6	0.00910	0.032760	1.636196
7	205.0495	515.6	0.00820	0.034669	1.681406
6	175.7567	515.6	0.00720	0.026729	1.265448
5	146.4640	515.6	0.00600	0.018562	0.878784
4	117.1712	515.6	0.00470	0.011390	0.550705
3	87.8784	515.6	0.00330	0.005615	0.289999
2	58.5856	515.6	0.00200	0.002062	0.117171
1	29.2928	515.6	0.00080	0.000330	0.023434
Σ	1000.0	4004.8		0.132116	6.443143

Table 1. Story displacements formed by fictional loads in the X direction

Thus, the total equivalent earthquake load is:

$$V_t = \frac{WA(T_1)}{R_a(T_1)} \ge 0.10. A_0 IW$$

$$V_{tx} = 2449.19 \text{ kN}$$

Similar to the calculations in the X direction, calculations were made for the Y direction, and V_{ty} was found as 2446.33 kN.

2.2.5. Equivalent earthquake loads acting on stories

According to the TBEC-2007 [19] Part 2.7.2, the total equivalent earthquake load on the top is expressed as the sum of the equivalent earthquake loads acting on all stories of the building. Accordingly, the equivalent earthquake load acting on the top N^{th} story (8th story) of the building was calculated with the following equations for the X and Y directions.

$$\Delta F_{NE}^{(X)} = 0.075 N V_{tE}^{(X)} = 146.95 \text{ kN}$$

$$\Delta F_{NE}^{(Y)} = 0.075 N V_{tE}^{(Y)} = 147.79 \text{ kN}$$

 $\Delta F_{NE}^{(X)}$ and $\Delta F_{NE}^{(Y)}$ additional equivalent earthquake forces were subtracted from the total equivalent earthquake forces and the remaining load was distributed to the stories for the X and Y directions with the help of Eq. (10).

$$F_{iE} = (V_{tE} - \Delta F_{NE}) \frac{m_i H_i}{\sum_{i=1}^{N} m_i H_i}$$
 (10)

Equivalent earthquake force calculations for X and Y directions are given below and the results of the calculations for all stories are presented in Table 2.

$$F_{iE}^{(X)} = (2449.19 - 146.95) \frac{m_i H_i}{\sum_{i=1}^{N} m_i H_i}$$

$$F_{iE}^{(Y)} = (2463.33 - 147.79) \frac{m_i H_i}{\sum_{j=1}^{N} m_i H_i}$$

2.2.6. Wind loads

Wind loads were calculated according to the terms specified in the standard named Effects on Structures - Part 1-4: General Effects - Wind Effects (TS EN 1991-1-4) [23]. Wind load distribution to the stories by surface width is presented in Table 3. The loads found were equally distributed to the stories by the SAP2000 [21] program.

2.2.7. Load combinations

Structural system load combinations were applied to the building according to the TBEC-2007 [19] and the RDCCPSS-2018 [22] as presented in Table 4.

Table 2. Equivalent seismic loads acting on stories

Story	$H_i(m)$	$m_i \times H_i (kNs^2)$	$\left(\frac{m_i*H_i}{\sum m_i*H_i}\right)$	$F_{iE}^{(X)}(kN)$	$F_{iE}^{(Y)}(kN)$
Roof	24	9494.4	0.179802	413.9470	416.3383
7	21	10827.6	0.205050	472.0733	474.8004
6	18	9280.8	0.175757	404.6342	406.9718
5	15	7734.0	0.146464	337.1952	339.1432
4	12	6187.2	0.117171	269.7561	271.3145
3	9	4640.4	0.087878	202.3171	203.4859
2	6	3093.6	0.058586	134.8781	135.6573
1	3	1546.8	0.029293	67.4390	67.8286
\sum		52804.8		2302.2400	2315.5400

Table 3. Distribution of wind load to the stories by surface width

Story	Height (m)	Wind Load for $b = 24 m$ (kN) $(1.14A_{ref})$	Wind Load for $b = 35 m$ (kN) $(1.14A_{ref})$
Roof	3	82.08	119.7
7	3	82.08	119.7
6	3	82.08	119.7
5	3	82.08	119.7
4	3	82.08	119.7
3	3	82.08	119.7
2	3	82.08	119.7
1	3	82.08	119.7
Σ	24	656.64	957.6

Table 4. Load combinations

$0.9G \pm EXN \pm 0.3EYN$	$G + Q \pm EXP \pm 0.3EYP$
$0.9G~\pm~0.3EXN~\pm~1.0EYN$	$G + Q \pm 0.3EXP \pm 1.0EYP$
$G + Q \pm EXP$	$G + Q \pm EXP \pm 0.3EYN$
$G + Q \pm EXN$	$G + Q \pm 0.3EXP \pm 1.0EYN$
$G + Q \pm EYP$	$G + Q \pm EXN \pm 0.3EYP$

Table 4. Continued	
$G + Q \pm EYN$	$G + Q \pm 0.3EXN \pm 1.0EYP$
$G + Q \pm E_X$	$G + Q \pm EXN \pm 0.3EYN$
$G + Q \pm E_Y$	$G + Q \pm 0.3EXN \pm 1.0EYN$
$0.9G \pm E_X$	$0.9G \pm EXP \pm 0.3EYP$
$0.9G \pm E_Y$	$0.9G~\pm~0.3EXP~\pm~1.0EYP$
$G + Q \pm W_X$	$0.9G \pm EXP \pm 0.3EYN$
$G + Q_R \pm W_Y$	$0.9G~\pm~0.3EXP~\pm~1.0EYN$
$0.9G \pm W_X$	$0.9G \pm EXN \pm 0.3EYP$
$0.9G~\pm W_Y$	$0.9G~\pm~0.3EXN~\pm~1.0EYP$
1.4G + 1.6Q	

where G is the dead load, Q is the live load, Q_R is the roof live load, E_X is the earthquake load in the X direction, E_Y is the earthquake load in the Y direction, E_XP denotes the X direction earthquake loading with +5% eccentricity, E_XP denotes the X direction earthquake loading with -5% eccentricity, E_XP denotes the Y direction earthquake loading with +5% eccentricity, and E_XP denotes the Y direction earthquake loading with -5% eccentricity, E_XP is the wind load in the Y direction, and E_XP is the wind load in the Y direction, and E_XP is the snow load.

2.2.8. Story drifts control

Control of the story drifts was performed according to the TBEC-2007 [19] earthquake code. Reduced story drift $(\Delta_i^{(X)})$, which expresses the displacement difference between two consecutive stories for any column or shear wall, is presented in Eq. (11).

$$\Delta_i^{(X)} = d_i^{(X)} - d_{i-1}^{(X)} \tag{11}$$

The values $d_i^{(X)}$ and $= d_{i-1}^{(X)}$ show the maximum lateral displacements calculated according to the reduced seismic loads at the ends of any column or shear wall at the i^{th} and $(i-1)^{th}$ stories of the building for the typical X earthquake direction.

According to the TBEC-2007 [19] Part 2.10.1.2, the effective story drift (δ_1) for the columns or shear walls at the ith story of the building for the typical X earthquake direction is given in Eq. (12), where R is the response reduction factor.

$$\delta_i^{(X)} = R \Delta_i^{(X)} \tag{12}$$

According to the TBEC-2007 [19] Part 2.10.1.3, for each earthquake direction, the maximum value of the effective story drifts (δ_l) calculated by Eq. (12) in the column or shear walls at any i^{th} story of the building must meet the following condition given in Eq. (13):

$$\frac{\delta_{i,max}^{(X)}}{h_i} \le 0.02$$

$$0.004 < 0.02$$
(13)

As a result of the calculations made, it was seen that the condition given in Eq. (13) was met for the X earthquake direction. The story drifts calculation values for the X earthquake direction are given in Table 5. The condition was also satisfied when the same calculations were performed for the Y earthquake direction.

Story	$H_i(m)$	$d_i^{(X)}(m)$	$\Delta_i^{(X)}(m)$	$\delta_i^{(X)}(m)$	$rac{\delta_{i,max}^{(X)}}{h_i}$
Roof	3	0.0162	0.0019	0.0095	0.003167
7	3	0.0143	0.0022	0.0110	0.003667
6	3	0.0121	0.0024	0.0120	0.004000
5	3	0.0097	0.0024	0.0120	0.004000
4	3	0.0073	0.0024	0.0120	0.004000
3	3	0.0049	0.0021	0.0105	0.003500
2	3	0.0028	0.0019	0.0095	0.003167
1	3	0.0009	0.0009	0.0045	0.001500

Table 5. The story drifts calculation for the X earthquake direction

2.2.9. Second order effects

In accordance with the TBEC-2007 [19] Part 2.10.2.1, the second order indicator value (Q_i) was calculated by Eq. (14) for each ith story for the earthquake direction considered and the necessary condition was checked for all stories.

$$\theta_i = \frac{(\Delta_i)_{ave} \sum_{j=i}^{N} w_j}{V_i h_i} \le 0.12$$
(14)

where w_j is the weight of the building's j^{th} story calculated using the live load participation coefficient. Second-order effects for the X earthquake direction are presented in Table 6. For the earthquake in the X direction, the maximum value of the Q_i parameters occurred at the 4^{th} story.

$$\Delta_4^{(X)} = 0.0023 m$$

$$\sum_{j=4}^{8} w_j = 4 * 5058 + 3881.6 = 24113.6 \text{ kN}$$

$$V_4^{(X)} = 413.947 + 472.0733 + 404.6342 + 337.1952 + 269.7561 = 1897.606 \text{ kN}$$

$$h_4 = 3 \text{ m}$$

$$\theta_i^{(X)} = \frac{\left(\Delta_i^{(X)}\right)_{ave} \sum_{j=i}^N w_j}{V_i^{(X)} h_i} = \frac{0.0023 * 24113.6}{1897.606 * 3} = 0.0097$$

The condition was satisfied. This condition was met when the same calculations were made for the other stories. Therefore, it was deduced that the second-order effects did not need to be considered. When the operations were repeated for the Y earthquake direction, it was concluded that the second-order effects did not require to be taken into account.

2.2.10. A1 torsional irregularity condition control

As stated in Table 2.1 of the TBEC-2007 [19] earthquake code, A1 torsional irregularity is expressed as the torsional irregularity coefficient (η_{bi}), which is the ratio of the maximum story drift at any story to the average story drift in the same direction at that story, being greater than 1.2 for each of the two perpendicular earthquake directions. The related Eq. is given as Eq. 15 below:

$$\eta_{bi} = \frac{(\Delta_i)max}{(\Delta_i)ave} > 1.2 \tag{15}$$

The η_{bi} values calculated for the structure are listed in Table 7. Since all the $\eta_{bi}(X)$ and the $\eta_{bi}(Y)$ values in Table 7 are less than 1.2, there is no A1 torsional irregularity in the building.

2.2.11. B2 stiffness irregularity condition control

B2 stiffness irregularity, as indicated in Table 2.1 of the TBEC-2007 [19], is defined as the stiffness irregularity coefficient (η_{ki}), which is defined by dividing the average story drift ratio at any floor other than the basement floors by the average story drift ratio in an upper or lower story for either of the two perpendicular earthquake directions, being more than 2.0. The (η_{ki}) values calculated for the structure are presented in Table 8. Since all the η_{ki} and η_{ki} values in Table 8 are less than 2.0, there is no B2 stiffness irregularity in the building.

Table 6. Second-order effects for the X earthquake direction

Story	$u_{i\ max}^{(X)}\left(m\right)$	$\Delta_{i \max}^{(X)}(m)$	$u_{i \ min}^{(X)}\left(m\right)$	$\Delta_{i \ min}^{(X)}(m)$	$\Delta_{i}^{(X)}_{ave}$
Roof	0.0162	0.0019	0.0142	0.0017	0.00180
7	0.0143	0.0022	0.0125	0.0019	0.00205
6	0.0121	0.0024	0.0106	0.0021	0.00225
5	0.0097	0.0024	0.0085	0.0020	0.00220
4	0.0073	0.0024	0.0065	0.0022	0.00230
3	0.0049	0.0021	0.0043	0.0018	0.00195
2	0.0028	0.0019	0.0025	0.0017	0.00180
1	0.0009	0.0009	0.0008	0.0008	0.00085

Table 7. A1 torsional irregularity condition control

Story	$\Delta_{i \max}^{(X)}(m)$	$\Delta_{i\ ave}^{(X)}$	${\eta_{bi}}_{(X)}$	$\Delta_{i \max}^{(Y)}(m)$	$\Delta_{i\ ave}^{(Y)}$	$\eta_{bi}{}_{(Y)}$
Roof	0.0019	0.00180	1.055556	0.0016	0.00155	1.032258
7	0.0022	0.00205	1.073171	0.0019	0.00180	1.055556
6	0.0024	0.00225	1.066667	0.0020	0.00195	1.025641
5	0.0024	0.00220	1.090909	0.0021	0.00195	1.076923
4	0.0024	0.00230	1.043478	0.0021	0.00205	1.024390
3	0.0021	0.00195	1.076923	0.0018	0.00170	1.058824
2	0.0019	0.00180	1.055556	0.0026	0.00215	1.209302
1	0.0009	0.00085	1.058824	0.0010	0.00095	1.052632

DD 11 0	D.OCC		11.1	
Table X	B2 stiffness	urregularity	condition	control
I doic o.	DZ BUILLION	, iii c z uiui it y	Condition	COIILIOI

Story	$\Delta_{i}^{(X)}_{ave}/h_{i}$	$\Delta_{i-1}_{ave}^{(X)}/h_{i-1}$	${\eta_{ki}}_{(X)}$	$\Delta_{i}^{(Y)}_{ave}/h_{i}$	$\Delta_{i-1}_{ave}^{(Y)}/h_{i-1}$	${\eta_{ki}}_{(Y)}$
Roof-7	0.000600	-	-	0.000517	-	-
7-6	0.000683	0.000683	0.878049	0.000600	0.000600	0.861111
6-5	0.000750	0.000750	0.911111	0.000650	0.000650	0.923077
5-4	0.000733	0.000733	1.022727	0.000650	0.000650	1.0
4-3	0.000767	0.000767	0.956522	0.000683	0.000683	0.951220
3-2	0.000650	0.000650	1.179487	0.000567	0.000567	1.205882

Table 9. Structural elements' dimensions

Structural System Elements	Cross-section profile according to the TBEC-2007 [19]
Columns	HE550B
Bracings	160*160*20
Beams	HE280B
Secondary Beams	IPE360

2.2.12. Dimensioning of the building according to the TBEC-2007 and the RDCCPSS-2018 principles The sections determined as a result of the calculations made for all the elements of the building by adhering to the TBEC-2007 [19] and the RDCCPSS-2018 [22] principles are presented in Table 9.

2.3. Design of the multi-story steel building according to the TBEC-2018 earthquake code

The design steps of the 8-story steel building consisting of concentrically braced steel frames by the Equivalent Static Method according to the TBEC-2018 [20] earthquake code are described in this section. The system periods, earthquake loads, lateral displacements, story drifts, irregularities, and dimensioning of the system elements were evaluated.

2.3.1. Vertical loads

The same vertical loads as the values used in the TBEC-2007 [19] design were utilized.

2.3.2. Earthquake characteristics

Earthquake characteristics are given as follows:

•	Local Soil Class:	ZB
•	Earthquake Ground Motion Level:	DD-2
•	Map Spectral Acceleration Coefficient for Short Period Region (S_s):	0.890
•	Map Spectral Acceleration Coefficient for 1.0 s Period (S_1):	0.244
•	Local Ground Effect Coefficient for Short Period Region (F_s) :	0.90
•	Local Ground Effect Coefficient for Short Period Region (F_1) :	0.80
•	Building Importance Factor (I):	1
•	Building Utilization Class (BKS)	3
•	Earthquake Design Class (DTS)	1

- Building Height Class (BYS) 5
- Structural System Behavior Coefficient (*R*): 5
- Excess Strength Coefficient (D) 2

2.3.3. Determination of the first natural vibration period of the building

According to the Equivalent Static Method in the TBEC-2018 [20] earthquake code, the first natural vibration periods of the building in both earthquake directions were calculated by Eq. (16).

$$T_1 = 2\pi \left(\frac{\sum_{i=1}^{N} m_i \, d_{fi}^2}{\sum_{i=1}^{N} F_{fi} d_{fi}} \right)^{1/2} \tag{16}$$

The value of the story mass, m_i , in Eq. (16) was found by using Eq. (17).

$$m_i = \frac{w_i}{g} = \frac{1}{g} [G_i + nQ_i] \tag{17}$$

The story weight and story mass of the first story were calculated as in Eq. (18), where n is taken as 30 for the first story according to Table 4.3 of the TBEC-2018 [20] earthquake code.

$$w_i = Area(G_n + n) + Perimeter(Q_n G_d)$$

$$w_i = (24 \times 35) \times (5.0 + 0.3 \times 2) + 2 \times (24 + 35) \times 3 = 5058 \, kN$$
(18)

$$m_i = 5058/9.81 = 515.6 \, kNs^2/m$$

Calculations were performed in the same way for other stories also. Fictive forces, F_{fi} , in the Eq. 4.26 of the TBEC-2018 [20], proportional to the story weights and the story heights were calculated by Eq. (19).

$$F_{fi} = F_0 \left(\frac{m_i H_i}{\sum_{j=1}^N m_j H_j} \right) \tag{19}$$

where, F_0 represents any chosen load and it was taken as 1000 kN. The F_{fi} forces in Table 10 were applied to story mass centers in the X and Y directions and story displacements were obtained by SAP2000 [21] program.

Table 10. Story	displacements	formed by	fictional l	oads in the	X direction

Story	$F_{fi}(kN)$	$m_i(kNs^2/m)$	$d_{fi(x)}(m)$	$m_i \times d_{fi(x)^2}$ (kNms²)	$F_{fi} \times d_{fi(x)} \ (kNm)$
Roof	179.8018	395.6	0.00910	0.032760	1.636196
7	205.0495	515.6	0.00820	0.034669	1.681406
6	175.7567	515.6	0.00720	0.026729	1.265448
5	146.4640	515.6	0.00600	0.018562	0.878784
4	117.1712	515.6	0.00470	0.011390	0.550705
3	87.8784	515.6	0.00330	0.005615	0.289999
2	58.5856	515.6	0.00200	0.002062	0.117171
1	29.2928	515.6	0.00080	0.000330	0.023434
\sum	1000.0	4004.8		0.132116	6.443143

Natural vibration periods $T_p^{(x)}$ and $T_p^{(y)}$ were calculated by Eq. (20).

$$T_p = 2\pi \left(\frac{\sum_{i=1}^{N} m_i \cdot d_{fi}^2}{\sum_{i=1}^{N} F_{fi} d_{fi}} \right)^{1/2}$$
 (20)

2.3.4. Total equivalent static lateral force calculation

The equivalent Static Lateral Force Method was applied because the BYS value was 5 and the DTS value was 1 for the structure designed according to TBEC-2018 [20] Part 4.6.2.2, and also because there were no torsion and B2 (soft story) irregularities in the structural system. In this case, the total equivalent earthquake load, V_{tE} , was calculated by Eq. (21).

$$V_{tE} = m_t \cdot S_{qR}(T) \ge 0.04 \cdot m_t \cdot I \cdot S_{DS} \cdot g \tag{21}$$

where m_t is the total mass of the upper part of the building above the basements, $S_{aR}(T)$ is the reduced design spectral acceleration, and S_{DS} is the short-period design spectral acceleration coefficient.

For the design spectral acceleration coefficients are defined in the Earthquake Hazard Maps and used for a location determined in Kilis, Türkiye.

$$S_{DS} = S_S. F_S = 0.801$$

The design spectral acceleration coefficient for a 1.0 s period, S_{D1} , is calculated as:

$$S_{D1} = S_1 \cdot F_1 = 0.195$$

Horizontal design spectrum corner period values are,

$$T_A = 0.2 \frac{S_{D1}}{S_{DS}} = 0.049 \, s$$

$$T_B = \frac{S_{D1}}{S_{DS}} = 0.244 \, s$$

The transition period to the constant displacement region, T_L , is:

$$T_{\rm L} = 6 s$$

Since $T_B = 0.244 \, s < T_p^{(X)} = 0.899 \, s < T_L = 6 \, s$, the horizontal elastic design spectral acceleration, $S_{ae}(T_p^{(X)})$, and the reduced design spectral acceleration, $S_{aR}(T_p^{(X)})$, is:

$$S_{ae}(T_p^{(X)}) = \frac{S_{D1}}{T_p^{(X)}} = \frac{0.195}{0.899} = 0.217$$

$$S_{aR}(T_p^{(X)}) = \frac{S_{ae}(T_p^{(X)})}{R_a(T_p^{(X)})} = \frac{0.217}{5} = 0.0434$$

where $R_a(T_p^{(X)})$ is the earthquake load reduction coefficient dependent on the projected ductility capacity and period.

$$V_{tE}^{(X)} = (4004.8)(0.0434 * 9,81) \ge 0.04.(4004.8)(10)(0.801)(9.81)$$

$$V_{tE}^{(X)} = 1705.06 \, kN \ge 1258.75 \, kN$$

Realizing the same operations for the Y direction also, $V_{tE}^{(Y)} = 1717.7 \ kN \ge 1258.75 \ kN$ was determined.

Story	$H_i(m)$	$m_i \times H_i (kNs^2)$	$\left(\frac{m_i*H_i}{\sum m_i*H_i}\right)$	$F_{iE}^{(X)}(kN)$	$F_{iE}^{(Y)}(kN)$
Roof	24	9494.4	0.179802	288.1792	290.3152
7	21	10827.6	0.205050	328.6452	331.0812
6	18	9280.8	0.175757	281.6959	283.7839
5	15	7734.0	0.146464	234.7466	236.4866
4	12	6187.2	0.117171	187.7973	189.1893
3	9	4640.4	0.087878	140.8479	141.8919
2	6	3093.6	0.058586	93.8986	94.5946
1	3	1546.8	0.029293	46.9493	47.2973
\sum		52804.8		1602.7600	1614.6400

Table 11. Equivalent seismic loads acting on stories

2.3.5. Equivalent earthquake loads acting on stories

The total equivalent earthquake load on the top is expressed as the sum of the equivalent earthquake loads acting on all stories of the building according to the TBEC-2018 [20] Part 4.7.2. Hence, the equivalent earthquake load acting on the top N^{th} story (8^{th} story) of the building was calculated with the following equations for the X and Y directions

$$\Delta F_{NE}^{(X)} = 0.0075 \, N \, V_{tE}^{(X)} = 0.0075 \times 8 \times 1705.06 = 102.3 \, kN$$

 $\Delta F_{NE}^{(Y)} = 0.0075 \, N \, V_{tE}^{(Y)} = 0.0075 \times 8 \times 1717.7 = 103.06 \, kN$

Additional equivalent earthquake forces $\Delta F_{NE}^{(X)}$ and $\Delta F_{NE}^{(Y)}$ were subtracted from the total equivalent earthquake forces and the remaining load was distributed to the stories with the help of Eq. (22) for the X and Y directions.

$$F_{iE} = (V_{tE} - \Delta F_{NE}) \frac{m_i H_i}{\sum_{j=1}^{N} m_i H_i}$$
 (22)

Equivalent earthquake force calculations for X and Y directions are presented below:

$$F_{iE}^{(X)} = (1705.06 - 102.3) \frac{m_i H_i}{\sum_{i=1}^{N} m_i H_i}$$

$$F_{iE}^{(Y)} = (1717.7 - 102.3) \frac{m_i H_i}{\sum_{j=1}^{N} m_i H_i}$$

The calculation results for all stories are given in Table 11.

2.3.6. Wind loads

Wind loads were calculated according to the terms specified in the TS EN 1991-1-4 [23] and they are the same as the values determined during the design of the structure according to the TBEC-2007 [19].

2.3.7. Load combinations

Structural system load combinations given in Table 12 were exerted on the structure according to the TBEC-2018 [20] and the RDCCPSS-2018 [22].

2.3.8. Story drifts control

The story drifts controls was realized according to the TBEC-2018 [20] Part 4.9.1. Reduced story drift $\Delta_i^{(X)}$, which is the difference between displacements of two consecutive stories for any column or shear wall, is given in Eq. (23).

$$\Delta_i^{(X)} = u_i^{(X)} - u_{i-1}^{(X)} \tag{23}$$

The values $u_i^{(X)}$ and $u_{i-1}^{(X)}$ designate the maximum lateral displacements determined according to the reduced seismic loads at the ends of any column or shear wall at the i^{th} and $(i-1)^{th}$ stories of the structure for the typical X earthquake direction. The effective story drift (δ i) for the columns or shear walls at the i^{th} story of the structure for the typical X earthquake direction according to the TBEC-2018 [20] Part 4.9.1.2 is given in Eq. (24).

$$\delta_i^{(X)} = \frac{R}{I} \Delta_i^{(X)} \tag{24}$$

The maximum value of the effective story drifts (δ i) calculated by Eq. (24) in the column or shear walls at any ith story of the building, for each earthquake direction, must satisfy the condition given in Eq. (25) according to the TBEC-2018 [20] Part 4.9.1.3:

$$\lambda \frac{\delta_{i,max}^{(X)}}{h_i} \le 0.008 \tag{25}$$

The coefficient λ is defined as the ratio of the elastic design spectral acceleration of the DD-3 earthquake to the elastic design spectral acceleration of the DD-2 earthquake, similar to the elastic design spectral acceleration of the DD-2 earthquake found previously, the elastic design spectral acceleration for the DD-3 earthquake is calculated as follows:

$$S_{ae}(T_p^{(X)})_{DD-3} = \frac{S_{D1}}{T_n^{(X)}} = \frac{0.066}{0.899} = 0.0734$$

$$S_{ae}(T_p^{(Y)})_{DD-3} = \frac{S_{D1}}{T_n^{(Y)}} = \frac{0.066}{0.892} = 0.0740$$

For each earthquake direction, the λ coefficients are determined as follows:

$$\lambda^{(X)} = \frac{S_{ae}(T_p^{(X)})_{DD-3}}{S_{ae}(T_p^{(X)})_{DD-2}} = \frac{0.0734}{0.217} = 0.338$$

$$\lambda^{(Y)} = \frac{S_{ae}(T_p^{(Y)})_{DD-3}}{S_{ae}(T_p^{(Y)})_{DD-2}} = \frac{0.074}{0.218} = 0.339$$

The story drifts calculation values for the X earthquake direction are presented in Table 13. As a result of the above calculations, it was seen that the condition given in Eq. (25) was fulfilled. The condition was also satisfied when the same calculations were made for the Y earthquake direction.

$$\lambda \frac{\delta_{i,max}^{(X)}}{h_i} = 0.001014 < 0.008 \quad \sqrt{}$$

Table 12. Load combinations

$0.9G \pm EXP \pm 0.3EYP$	$1.2G + 1.6Q_R$
$0.9G~\pm~0.3EXP~\pm~1.0EYP$	1.2G + 1.6S
$0.9G + EXP \pm 0.3EYN$	$1.2G + 1.6Q + 0.5Q_R$
$0.9G \pm 0.3EXP \pm 1.0EYN$	1.2G + 1.6Q + 0.5S
$0.9G \pm EXN \pm 0.3EYP$	$1.2G + 1.6Q_R + 1.0Q$
$0.9G \pm 0.3EXN \ \pm \ 1.0EYP$	1.2G + 1.6S + 1.0Q
$0.9G \pm EXN \pm 0.3EYN$	$1.2G + 1.0Q + 0.2S \pm EXP \pm 0.3EYP$
$0.9G \pm 0.3EXN \ \pm \ 1.0EYN$	$1.2G + 1.0Q + 0.2S \pm 0.3EXP \pm 1.0EYP$
$1.2G + 1.6Q_R \pm 0.8W_X$	$1.2G + 1.0Q + 0.2S \pm EXP \pm 0.3EYN$
$1.2G + 1.6Q_R \pm 0.8W_Y$	$1.2G + 1.0Q + 0.2S \pm 0.3EXP \pm 1.0EYN$
$1.2G + 1.0Q + 0.5Q_R \pm 1.6W_X$	$1.2G + 1.0Q + 0.2S \pm EXN \pm 0.3EYP$
$1.2G + 1.0Q + 0.5Q_R \pm 1.6W_Y$	$1.2G + 1.0Q + 0.2S \pm 0.3EXN \pm 1.0EYP$
$0.9G \pm 1.6W_X$	$1.2G + 1.0Q + 0.2S \pm EXN \pm 0.3EYN$
$0.9G~\pm~1.6W_Y$	$1.2G + 1.0Q + 0.2S \pm 0.3EXN \pm 1.0EYN$
1.4G	

Table 13. The story drifts calculation for the X earthquake direction

Story	$H_i(m)$	$u_i^{(X)}(m)$	$\Delta_i^{(X)}(m)$	$\delta_i^{(X)}(m)$	$\lambda rac{\delta_{i,max}^{(X)}}{h_i}$
Roof	3	0.0120	0.0013	0.0065	0.000732
7	3	0.0107	0.0015	0.0075	0.000845
6	3	0.0092	0.0016	0.0080	0.000901
5	3	0.0076	0.0018	0.0090	0.001014
4	3	0.0058	0.0017	0.0085	0.000958
3	3	0.0041	0.0017	0.0085	0.000958
2	3	0.0024	0.0015	0.0075	0.000845
1	3	0.0009	0.0009	0.0045	0.000507

2.3.9. Second-order effects

The second-order indicator value $(\theta_{II,i}^{(X)})$ for each i^{th} story for the X earthquake direction was found by Eq. (26) according to the TBEC-2018 [20] Part 4.9.2.

$$\theta_{II,i}^{(X)} = \frac{\left(\Delta_i^{(X)}\right)_{ave} \sum_{k=i}^{N} w_k}{V_i^{(X)} h_i}$$
 (26)

 $\theta_{II,max}^{(X)}$ which is the maximum value of the $\theta_{II,i}^{(X)}$ calculated for all stories is presented in Eq. (27).

$$\theta_{II,max}^{(X)} \le 0.12 \frac{D}{C_h R} \tag{27}$$

where C_h is a coefficient defined depending on the nonlinear hysteretic behavior of the structural system, whose value is taken as equal to 1 in steel buildings.

According to the TBEC-2018 [20] Part 4.9.2.2, it is stated that if the condition given in Eq. (19) is met, it is not necessary to take into account the second-order effects in the calculation of the internal forces in the design. Second-order effects for the X earthquake direction are presented in Table 14. The maximum value of the θ_{ILi} parameters took place at the 5th story for the earthquake in the X direction.

$$\Delta_{5}^{(X)}{}_{ave} = 0.00165 m$$

$$\sum_{j=5}^{8} w_j = 3 * 5058 + 3881.6 = 19055.6 kN$$

$$V_5^{(X)} = 288.18 + 328.64 + 281.69 + 234.74 = 1133.26 kN$$

$$h_5 = 3 m$$

$$\theta_{II,i}^{(X)} = \frac{\left(\Delta_{i}^{(X)}\right)_{ave} \sum_{k=i}^{N} w_k}{V_i^{(X)} h_i} = \frac{0.00165 * 19055.6}{1133.26 * 3} = 0.00925$$

When the values were substituted in Eq. 27:

$$0.00925 \le 0.12 \frac{2}{1*5} = 0.048$$

the condition was satisfied. Therefore, it was not necessary to consider the second-order effects. When the operations were repeated for the Y earthquake direction, it was concluded that the second-order effects did not need to be considered.

2.3.10. A1 torsional irregularity condition control

A1 torsional irregularity is defined as the torsional irregularity coefficient (η_{bi}), which expresses the ratio of the maximum story drift at any story to the mean story drift in the same direction at that story, being greater than 1.2 for each of the two perpendicular earthquake directions, as indicated in the TBEC-2018 [20] Table 3.6. The torsional irregularity coefficient is calculated by Eq. (28).

$$\eta_{bi} = \frac{(\Delta_i)max}{(\Delta_i)ave} > 1.2 \tag{28}$$

The η_{bi} values calculated for the structure are presented in Table 15. Since all the $\eta_{bi(X)}$ and the $\eta_{bi(Y)}$ values in Table 13 are less than 1.2, there is no A1 torsional irregularity in the building.

2.3.11. B2 stiffness irregularity condition control

B2 stiffness irregularity is defined as the stiffness irregularity coefficient η_{ki} being more than 2.0, which is defined by dividing the average story drift ratio at any i^{th} story, excluding basement floors, by the average story drift ratio in an upper or lower story for either of the two perpendicular earthquake directions, as stated in Table 3.6 of the TBEC-2018 [20]. The η_{ki} values calculated for the building are given in Table 16. Since all the η_{ki} and η_{ki} values in Table 14 are less than 2.0, there is no B2 stiffness irregularity in the building.

Table 14. Second-order effects for the X earthquake direction

Story	$u_{i\ max}^{(X)}\left(m\right)$	$\Delta_{i \max}^{(X)}(m)$	$u_{i \ min}^{(X)}\left(m \right)$	$\Delta_{i \ min}^{(X)}(m)$	$\Delta_{i}^{(X)}_{ave}$
Roof	0.0120	0.0013	0.0102	0.0010	0.00115
7	0.0107	0.0015	0.0092	0.0013	0.00140
6	0.0092	0.0016	0.0079	0.0014	0.00150
5	0.0076	0.0018	0.0065	0.0015	0.00165
4	0.0058	0.0017	0.0050	0.0015	0.00160
3	0.0041	0.0017	0.0035	0.0014	0.00155
2	0.0024	0.0015	0.0021	0.0014	0.00145
1	0.0009	0.0009	0.0007	0.0007	0.00080

Table 15. A1 torsional irregularity condition control

Story	$\Delta_{i \max}^{(X)}(m)$	$\Delta_{i \ ave}^{(X)}$	$\eta_{bi}{}_{(X)}$	$\Delta_{i \max}^{(Y)}(m)$	$\Delta_{i}^{(Y)}_{ave}$	$\eta_{bi}{}_{(Y)}$
Roof	0.0013	0.00115	1.130435	0.0011	0.00105	1.047619
7	0.0015	0.00140	1.071429	0.0013	0.00130	1.0
6	0.0016	0.00150	1.066667	0.0015	0.00140	1.071429
5	0.0018	0.00165	1.090909	0.0016	0.00155	1.032258
4	0.0017	0.00160	1.062500	0.0016	0.00155	1.032258
3	0.0017	0.00155	1.096774	0.0015	0.00145	1.034483
2	0.0015	0.00145	1.034483	0.0015	0.00140	1.071429
1	0.0009	0.00080	1.125000	0.0010	0.00095	1.052632

Table 16. B2 stiffness irregularity condition control

Story	$\Delta_{i}^{(X)}_{ave}/h_{i}$	$\Delta_{i-1_{ave}}^{(X)}/h_{i-1}$	$\eta_{_{ki}{_{(X)}}}$	${\Delta_i^{(Y)}}_{ave}/h_i$	$\Delta_{i-1_{ave}}^{(Y)}/h_{i-1}$	$\eta_{_{ki}{_{(Y)}}}$
Roof-7	0.000383	-	-	0.000350	-	-
7-6	0.000467	0.000467	0.821429	0.000433	0.000433	0.807692
6-5	0.000500	0.000500	0.933333	0.000467	0.000467	0.928571
5-4	0.000550	0.000550	0.909091	0.000517	0.000517	0.903226
4-3	0.000533	0.000533	1.031250	0.000517	0.000517	1.0
3-2	0.000517	0.000517	1.032258	0.000483	0.000483	1.068966
2-1	0.000483	0.000483	1.068966	0.000467	0.000467	1.035714
1-Basement	-	0.000267	1.812500	-	0.000317	1.473684

2.3.12. Dimensioning of the building according to the TBEC-2018 and the RDCCPSS-2018 principles The sections specified as a result of the calculations performed for all the elements of the structure according to the TBEC-2018 [20] and the RDCCPSS-2018 [22] bases are given in Table 17.

Table 17. Dimension of the structural of	elements
Structural system elements	Cross-section profile according to the TBEC-2018 [20]
Columns	HE500B
Bracings	120*120*17.5
Beams	HE300B
Secondary Beams	IPE360

3. Comparison and evaluation of the results

In the research, an 8-story steel building with a high ductility level in both directions and composed of concentrically braced steel frames were designed according to the TBEC-2007 [19] and the TBEC-2018 [20] earthquake codes, the designs were compared, and the system was dimensioned in accordance with the RDCCPSS-2018 [22] principles.

While designing the structure according to the TBEC-2007 [19] and the TBEC-2018 [20] earthquake codes, the dominant natural vibration periods of the building, base shear forces, equivalent earthquake loads lateral displacements, the story drifts, second-order effects, A1 type torsional irregularities, B2 type stiffness irregularities were examined, and the dimensions of the elements as a result of the most unfavorable loading were determined. The Equivalent Static Method was utilized while designing according to both earthquake codes. To observe the effects of the earthquake code difference on the designs, the following comparisons were performed:

3.1. Comparison of the structural system periods

As a result of the calculations pursued according to the bases of the TBEC-2007 [19] and the TBEC-2018 [20], it was observed that the values of the structural system periods in the X and the Y earthquake directions remained the same since the calculation steps are the same for both earthquake codes.

3.2. Comparison of the story displacements formed by fictional loads

The story displacements obtained by fictional loads in the X direction calculated according to the TBEC-2007 [19] and the TBEC-2018 [20] earthquake codes were equal. The displacements in the Y direction with respect to both codes were also the same. The story displacements in the X and Y directions are demonstrated in Fig. 5.

3.3. Comparison of the equivalent seismic loads acting on stories

The equivalent earthquake loads determined by utilizing Equivalent Static Method according to the TBEC-2007 [19] and the TBEC-2018 [20] earthquake codes' principles for the X and Y directions are compared in Figs. 6 and 7, respectively.

When the sum of the equivalent earthquake loads acting on stories was examined, it was seen that the results found according to the TBEC-2007 [19] bases were considerably higher than the results got according to the TBEC-2018 [20] principles. The cause of this variance can be explained as the difference in the defined earthquake loads.

3.4. Comparison of the story drifts

The story drifts determined according to the TBEC-2007 [19] and the TBEC-2018 [20] earthquake codes for the X and Y directions are compared in Figs. 8 and 9, respectively. It was seen that the story drift values found for the X and the Y earthquake directions did not exceed the limit states. For this reason, it was not considered necessary to increase the rigidity of the structural system.

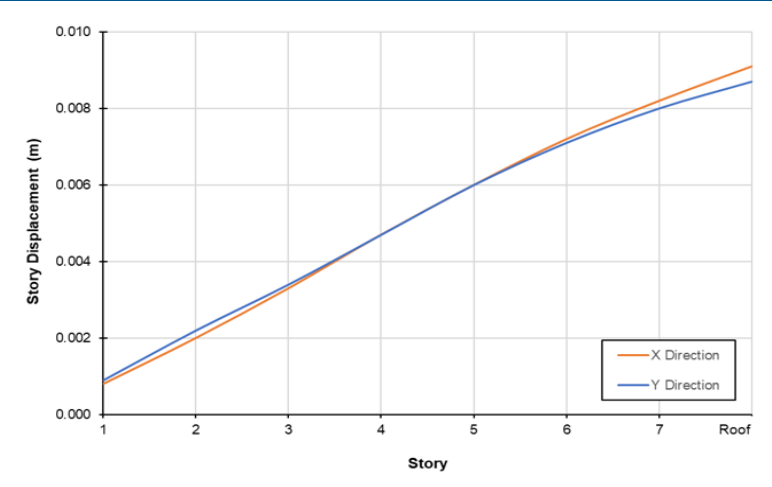


Fig. 5. Story displacements in the X and Y directions according to the TBEC-2007 [19] and the TBEC-2018 [20]

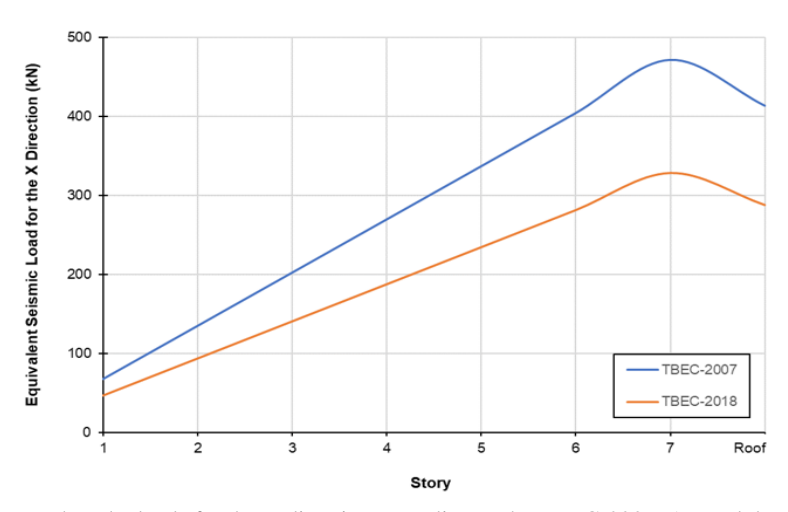


Fig. 6. Equivalent earthquake loads for the X direction according to the TBEC-2007 [19] and the TBEC-2018 [20]

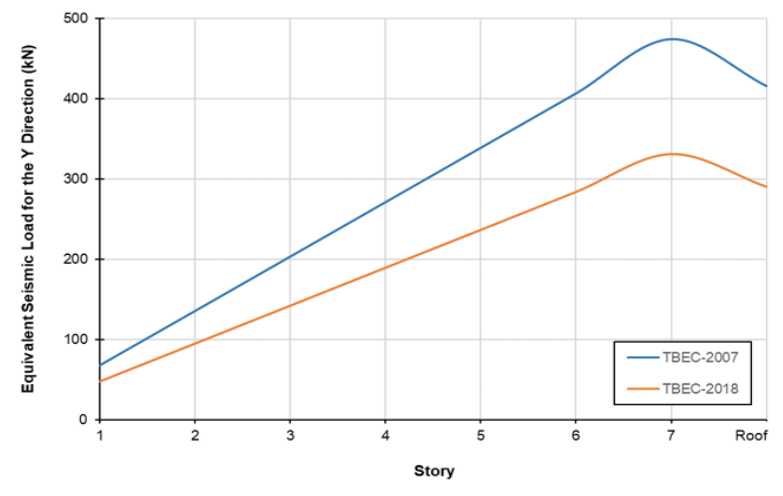


Fig. 7. Equivalent earthquake loads for the Y direction according to the TBEC-2007 [19] and the TBEC-2018 [20]

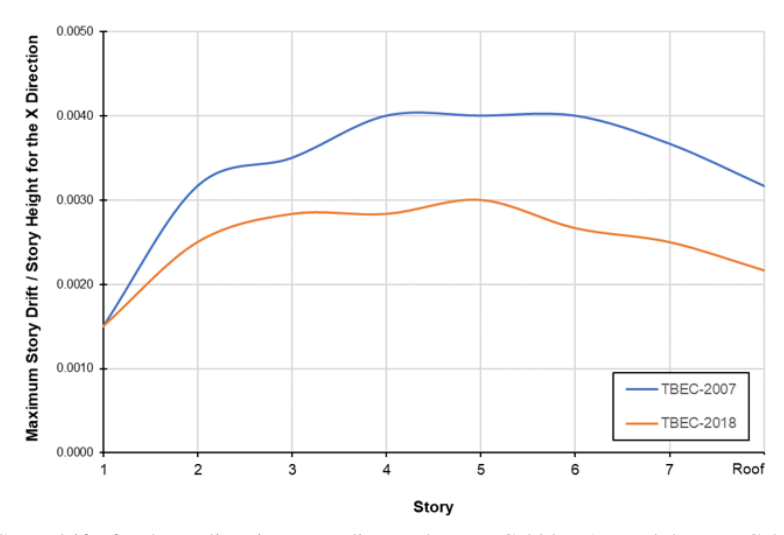


Fig. 8. Story drifts for the X direction according to the TBEC-2007 [19] and the TBEC-2018 [20]

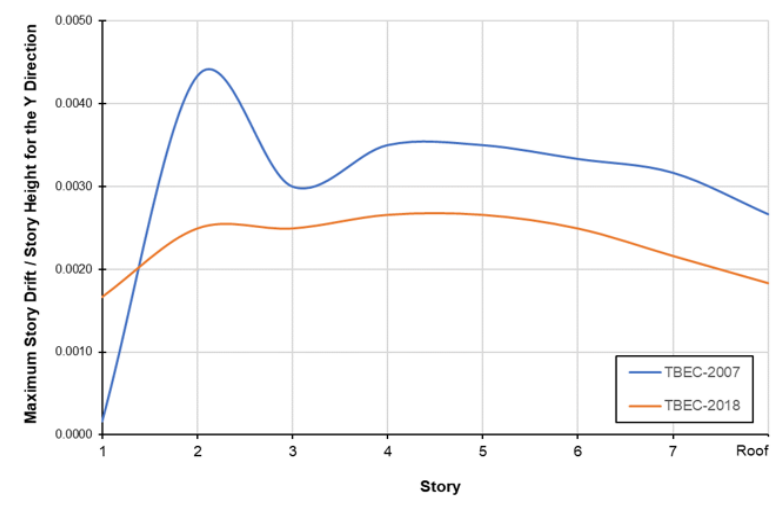


Fig. 9. Story drift rifts for the Y direction according to the TBEC-2007 [19] and the TBEC-2018 [20]

3.5. Comparison of the A1 torsional irregularity condition

The results obtained from the A1 torsional irregularity condition controls according to the TBEC-2007 [19] and the TBEC-2018 [20] earthquake codes for the X and Y directions are presented in Figs. 10 and 11, respectively.

3.6. Comparison of the B2 stiffness irregularity condition

The results acquired from the B2 stiffness irregularity condition controls according to the TBEC-2007 [19] and the TBEC-2018 [20] earthquake codes for the X and Y directions are given in Figs. 12 and 13, respectively. When the results of the irregularity conditions control in Figs. 10-13 are evaluated, and it is observed that there is no irregularity in the structure according to the TBEC-2007 [19] and the TBEC-2018 [20] principles. The results of the irregularity controls according to the TBEC-2007 [19] bases were higher than the results obtained according to the TBEC-2018 [20] principles. The reason for this result was that earthquake loads found according to the TBEC-2007 [19] were greater than the ones determined according to the TBEC-2018 [20].

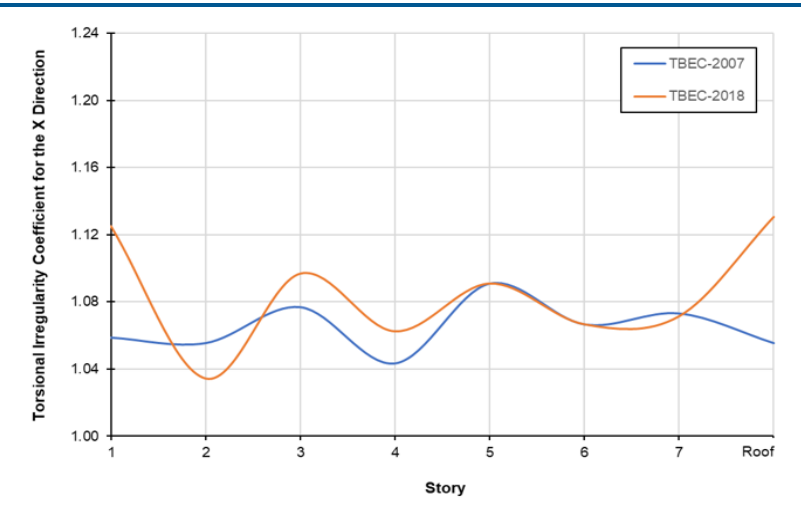


Fig. 10. A1 torsional irregularity condition control for the X direction according to the TBEC-2007 [19] and the TBEC-2018 [20]

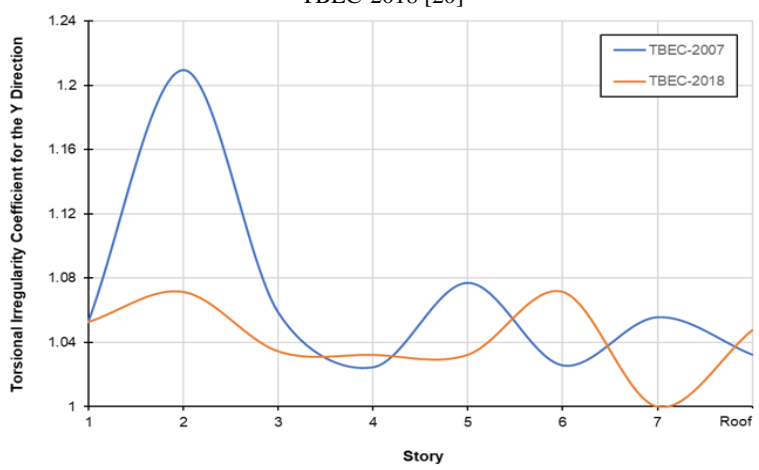


Fig. 11. A1 torsional irregularity condition control for the Y direction according to the TBEC-2007 [19] and the TBEC-2018 [20]

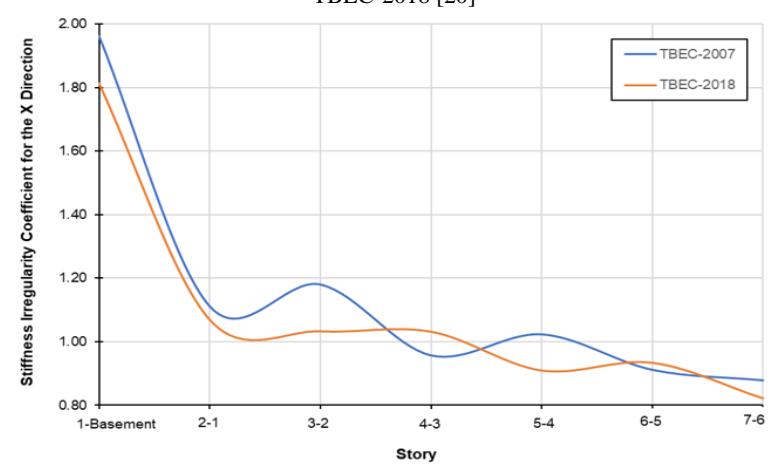


Fig. 12. B2 stiffness irregularity condition control for the X direction according to the TBEC-2007 [19] and the TBEC-2018 [20]

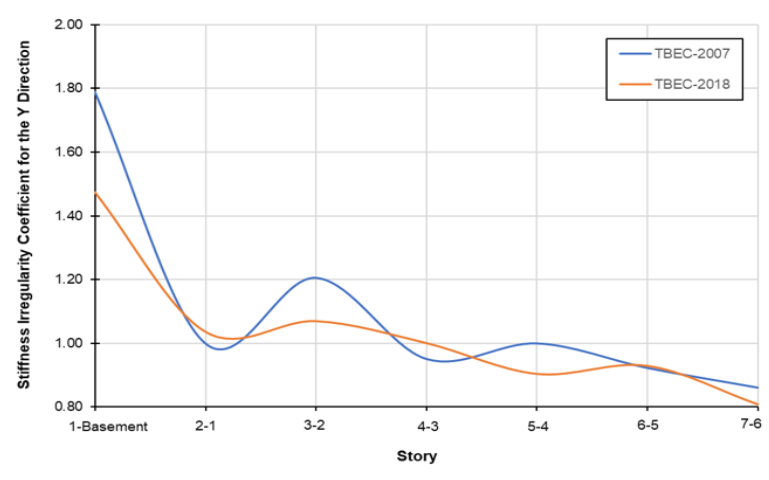


Fig. 13. B2 stiffness irregularity condition control for the Y direction according to the TBEC-2007 [19] and the TBEC-2018 [20]

Table 18. Dimensions of the system elements according to the TBEC-2007 [19] and the TBEC-2018 [20]

Structural system elements	Cross-section profile according to the TBEC-2007 [19]	Cross-section profile according to the TBEC-2018 [20]
Columns	HE550B	HE500B
Bracings	160*160*20	120*120*17.5
Beams	HE280B	HE300B
Secondary Beams	IPE360	IPE360

3.7. Comparison of the structural elements' dimensions

The cross-section profiles determined as a result of dimensioning of the structure according to the TBEC-2007 [19] and the TBEC-2018[20] bases are presented in Table 18. From an economic point of view, it was observed that a structure designed according to the TBEC-2018 [20] principles is more advantageous than a structure designed according to the TBEC-2007 [19] bases.

4. Concluding remarks

In this research, the TBEC-2007 [19] and the TBEC-2018 [20] earthquake codes were comprehensively examined. Moreover, the effects of the earthquake code differences on the structural system periods, earthquake loads, lateral displacements, story drifts, second-order effects, irregularities, and dimensioning of the elements in the structure were studied in detail on an 8-story steel building of high ductility level in both directions and having concentrically braced steel frames. The Equivalent Static Method was used during the design of the building according to both earthquake codes. While dimensioning the structural elements, the RDCCPSS-2018 [22] principles were followed and the LRFD Method was utilized. For the analyses of the 8-story steel building according to both earthquake codes, SAP2000 [21] structural analysis program was used.

Although steel structures have many advantages against earthquakes, there is a fact that multi-story buildings in Türkiye are commonly of reinforced concrete and the studies performed are mostly on reinforced concrete structures. Hence, there is a lack of research on the multi-story steel structures topic. There existed no study on the design of multi-story steel structures based on the TBEC-2007 [19] and the TBEC-2018 [20] earthquake codes at the time of the research. For this reason, the research has high originality value.

The variances observed between the TBEC-2007 [19] and the TBEC-2018 [20] earthquake codes during the analysis and design phases and the calculation results can be summarized as follows:

- The TBEC-2018 [20] earthquake code gives more precise results in defining the earthquake load since
 it directly depends on the coordinates of the area where the building will be built, while TBEC-2007
 [19] uses a more general approach based on determining the earthquake load by the earthquake zone
 of the place.
- 2. The TBEC-2018 [20] offers more sensitive ground options than the TBEC-2007 [19] principles, hence it allows more precise calculations. On the other hand, more general assumptions are made according to the TBEC-2007 [19] earthquake code.
- 3. While making a design, BYS is selected according to the height of the building in the TBEC-2018 [20] code. Whereas, there is no such classification in the TBEC-2007 [19] earthquake code.
- 4. Greater base shear forces were obtained while designing according to the TBEC-2007 [19] code due to the differences in the defined earthquake loads according to both earthquake codes. Moreover, during the dimensioning of the structural elements for the most unfavorable conditions, larger sections were found according to the TBEC-2007 [19] earthquake code, the structure remained very safe, and it was far from being economical.
- 5. Moreover, it has been made obligatory to apply deformation-based design for high-rise buildings in the TBEC-2018 [20] earthquake code.
- 6. Besides these, there exist no significant differences in the calculations of the building importance factor, natural vibration period, story drifts, and structural irregularities in both earthquake codes.

The conclusions are drawn as a result of the calculations pursued according to the TBEC-2007 [19] and the TBEC-2018 [20] earthquake codes during the analysis and design of the 8-story steel building can be listed below:

- 1. The values of the structural system periods in the X and Y directions were observed to be the same since the calculation steps are the same in both codes.
- 2. The story displacements obtained by fictional loads in the X direction calculated according to the TBEC-2007 [19] and the TBEC-2018 [20] earthquake codes were equal. The same was true for the Y direction also.
- 3. When the sum of the equivalent earthquake loads acting on stories was investigated, it was seen that the results obtained according to the TBEC-2007 [19] were considerably higher than the ones gathered according to the TBEC-2018 [20] principles. The reason for this difference can be explained as the variance in the defined earthquake loads.
- 4. Moreover, it was seen that the story drift values obtained for the X and Y directions did not pass the limit states. For this reason, it was not considered necessary to increase the rigidity of the system.
- 5. Also, it was seen that there was no irregularity in the structure according to the TBEC-2007 [19] and the TBEC-2018 [20] bases. The results of the irregularity controls according to the TBEC-2007 [19] principles were higher than the results obtained according to the TBEC-2018 [20]. The reason for this was the fact that earthquake loads found according to the TBEC-2007 [19] were greater than the ones determined according to the TBEC-2018 [20].
- 6. From an economic perspective, it was seen that a structure designed according to the TBEC-2018 [20] principles is more advantageous than a structure designed according to the TBEC-2007 [19].

Further studies can be carried out on rigid frame systems, eccentrically braced systems, or steel systems with limited ductility, and the codes can be compared. The Equivalent Earthquake Load Method, which is a strength-based design method, was used to design the 8-story steel building in the research. The study can also be performed using the other strength-based design methods, the Mode Combination Method and the Mode Addition Method in the Time History. In addition; in future studies, analysis and dimensioning can be

realized by using the deformation-based methods, Single or Multi-Mode Pushover Methods, and Non-Linear Calculation Methods in the Time Domain.

Conflict of interests

The author(s) declared no potential conflicts of interest with respect to the research, authorship, and/or publication of this article.

Funding

This research received no external funding.

Data availability statement

No new data were created or analyzed in this study.

References

- [1] Çırpan B (2017) The Effect of Structural Geometry on Structural System Behavior in Multi-Story Steel Structures and Determination of the Ideal Geometric Form, M.Sc. Thesis, Pamukkale University, Denizli, Türkiye.
- [2] Tremblay R, Poncet L (2005) Seismic performance of concentrically braced steel frames in multistory buildings with mass irregularity. Journal of Structural Engineering 131(9).
- [3] Uriz P, Mahin SA (2004) Seismic performance assessment of concentrically braced steel frames. In: Proceedings of World Conference on Earthquake Engineering. Vancouver, BC, Canada
- [4] Qiu C-X, Zhu S (2016) High-mode effects on seismic performance of multi-story self-centering braced steel frames. Journal of Constructional Steel Research 119(2016):133-143.
- [5] Chao S-H, Karki NB, Sahoo DR (2012) Seismic behavior of steel buildings with hybrid braced frames. Journal of Structural Engineering 139(6).
- [6] Shen J, Seker O, Akbas B, Seker P, Momenzadeh S, Faytarouni M (2017) Seismic performance of concentrically braced frames with and without brace buckling. Engineering Structures 141(2017):461-481.
- [7] Avcı N, Alemdar F (2019) Shaking table test and numerical simulation of 3D steel frame system. Journal of Structural Engineering & Applied Mechanics 2(2):88-95.
- [8] Annan CD, Youssef MA, El Naggar MH (2009) Experimental evaluation of the seismic performance of modular steel-braced frames. Engineering Structures 31(2009):1435-1446.
- [9] Kirruti P, Pekrioglu Balkis A (2020) Seismic performance assessment of steel bracing systems in high-rise reinforced concrete structures. Journal of Structural Engineering & Applied Mechanics 3(2):110-126.
- [10] Serttaş T (2014) Design of a Multi-Story Steel Building According to İstanbul High Buildings Earthquake Code and AISC 360.10, M.Sc. Thesis, İstanbul Teknik University, İstanbul, Türkiye.
- [11] Yousuf MD, Bagchi A (2009) Seismic design and performance evaluation of steel-frame buildings designed using the 2005 national building code of Canada. Canadian Journal of Civil Engineering 36:280-294.
- [12] Yousuf MD, Bagchi A (2010) Seismic performance of a 20-story steel-frame building in Canada. The Structural Design of Tall and Special Buildings 19: 901-921.
- [13] Nakai M, Koshika N, Hirakawa KK, Wada A (2012) Performance-based seismic design for high-rise buildings in Japan. International Journal of High-Rise Buildings 1:155-167.
- [14] Nateghi EF, Rezaei-Tabrizi A (2013) Nonlinear dynamic response of tall buildings considering soil-structure effects. The Structural Design of Tall and Special Buildings 22:1075-1082.
- [15] Dağdeviren A (2013) Performance Based Design Principles and Investigation of Nonlinear Behavior in Multi-Story Steel Structures, M.Sc. Thesis, Yıldız Teknik University, İstanbul, Türkiye.
- [16] Atalay ÖB (2021) Performance Comparison of Eccentrical and Concentrical Braced Steel Frame Structures with the Non-Linear Push-Over Analysis Method, M.Sc. Thesis, İstanbul Technical University, İstanbul, Türkiye.
- [17] Kor E, Ozcelik Y (2022) Seismic performance assessment of concentrically braced steel frames designed to the Turkish Building Earthquake Code 2018. Structures 40:759-770.

[18] Yıldızhan Sağer B, Temel B (2022) Moment aktaran ve merkezi çaprazlı çok katlı çelik yapıların 2018 Türkiye Bina Deprem Yönetmeliğine göre analizi ve tasarımı (TBDY-2018). Cukurova University Journal of the Faculty of Engineering 37:1017-1030 (in Turkish).

- [19] TBEC-2007 (2007) Regulation on Buildings to be Constructed in Earthquake Zones. Ministry of Public Works and Settlement, Ankara, Türkiye.
- [20] TBEC-2018 (2018) Turkish Building Earthquake Code. Disaster and Emergency Management Presidency, Ankara, Türkiye.
- [21] Computers and Structures Inc. SAP2000: Integrated Software for Structural Analysis and Design. Berkeley, CA, US.
- [22] RDCCPSS-2018 (2018) Regulation on Design, Calculation, and Construction Principles of Steel Structures. Ministry of Environment and Urbanization, Ankara, Türkiye.
- [23] Turkish Standardization Institute (2007) TS EN 1991-1-4: Effects on Structures Part 1-4: General Effects-Wind Effects. Ankara, Türkiye.